ACS Sustainable Chemistry & Engineering

pubs.acs.org/journal/ascecg

Research Article

Ethanol Electro-oxidation Reaction Selectivity on Platinum in Aqueous Media

Rubén Rizo, Adolfo Ferre-Vilaplana,* Enrique Herrero,* and Juan M. Feliu

Cite This: *ACS Sustainable Chem. Eng.* 2023, 11, 4960−4968

Read Online

ACCESS | Metrics & More | Article Recommendations | Supporting Information

ABSTRACT: Ethanol fuel cells require selective catalysts for complete oxidation of the fuel, which involves C−C bond cleavage. From experiments on well-defined surfaces and calculations, the mechanism controlling the ethanol electro-oxidation selectivity on platinum in aqueous media as a model system is elucidated. Adsorbed OH favors ethanol adsorption and conversion into adsorbed ethoxy, which favorably evolves to adsorbed $COCH_3$. On Pt(111), adsorbed OH is also readily incorporated into adsorbed $COCH_3$ to yield acetic acid. A higher barrier for this latter step on Pt(100) enables the $COCH_3$ dehydrogenation to adsorbed $COCH_2$, favoring C−C bond cleavage. As adsorbed OH plays an essential role as a reactant in this process, its adsorption properties have a decisive impact on this reaction. Furthermore, the adsorbed OH diffusion rate on the surface, which depends on the adsorbate/media/surface interaction at the interface, modulates the availability of this key reactant. These results highlight that the search for selective electrocatalysts requires holistic consideration of reactants, adsorbates, media, and substrate.

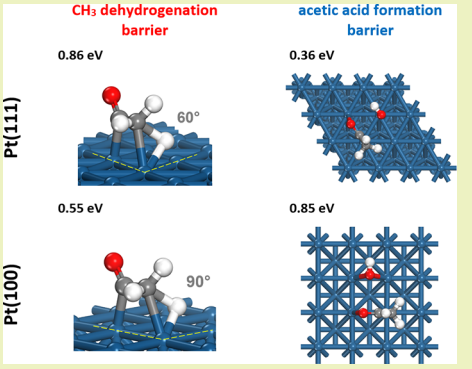

KEYWORDS: *Electrocatalysis, Selectivity, Ethanol oxidation, Adsorbed OH, Platinum, Density-functional theory calculations*

INTRODUCTION

Stored energy is required to power devices (from cell phones to vehicles) as well as to cope with the intermittence of renewable sources (from the daily intermittence of photovoltaics to major episodes of renewable contribution shortage).[1−4] Energy can be efficiently stored in batteries, although fuels have higher energy densities.[5] Moreover, while batteries must be scaled for both power and capacity, fuel cells can be scaled for power only. As a result, frequent demands of small capacities can be met more effectively by batteries, but fuels can be more effective when large capacities are episodically required. Thus, both batteries and fuels should play a role in the future energy storage landscape.

Hydrogen has, by far, the highest specific energy density among fuels, although alcohols have larger volumetric energy densities and are more easily stored. Being the simplest alcohol having C−C bonds, ethanol has a higher specific and volumetric energy density than methanol. It is also less toxic, and it can be readily produced under CO_2 neutral conditions from biomass.[6] Moreover, CO_2 conversion into ethanol is also being investigated.[7−10] Thus, ethanol can play a role as an energy vector. The energy stored in ethanol can be recovered by combustion as well as by electro-oxidation in fuel cells, even though large overpotentials are required to oxidize alcohols.[11]

Complete oxidation of ethanol to CO_2 involves C−C bond cleavage and CO formation as well as exchange of 12 electrons, but acetic acid can be also produced as a final product, exchanging only 4 electrons.[11] Thus, to maximize the energy recovered from ethanol, selective electrocatalysts for complete oxidation of the fuel are required. Despite platinum being the best pure metal anode to oxidize ethanol under acidic conditions, its selectivity for CO_2 is still low[12] and strongly depends on the surface structure of the electrode. Pt(111) exhibits nearly 100% selectivity toward the formation of acetic acid.[13,14] In fact, studies on stepped surfaces having (111) symmetry terraces have revealed that C−C bond cleavage takes place only on the steps.[14,15] Thus, the CO_2 traces measured during ethanol oxidation on real Pt(111) electrodes should be attributed to the presence of defects. By contrast, Pt(100) gives rise to the highest production of CO_2 during this electro-oxidation process, although a higher onset potential is required on this surface.[13] The formation of acetic acid not only implies a loss in the energy recovered from the fuel but also hinders ethanol oxidation since acetate remains strongly adsorbed by both oxygen atoms of the carboxylic group on these electrodes.[13,16] Studies on the formic acid and methanol oxidations on this metal have revealed that these electrocatalytic reactions require not only the adsorption and activation of reactants in the right configuration but also the

Received: May 4, 2022
Revised: June 27, 2022
Published: July 12, 2022

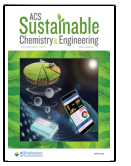

https://doi.org/10.1021/acssuschemeng.2c02663
ACS Sustainable Chem. Eng. 2023, 11, 4960−4968

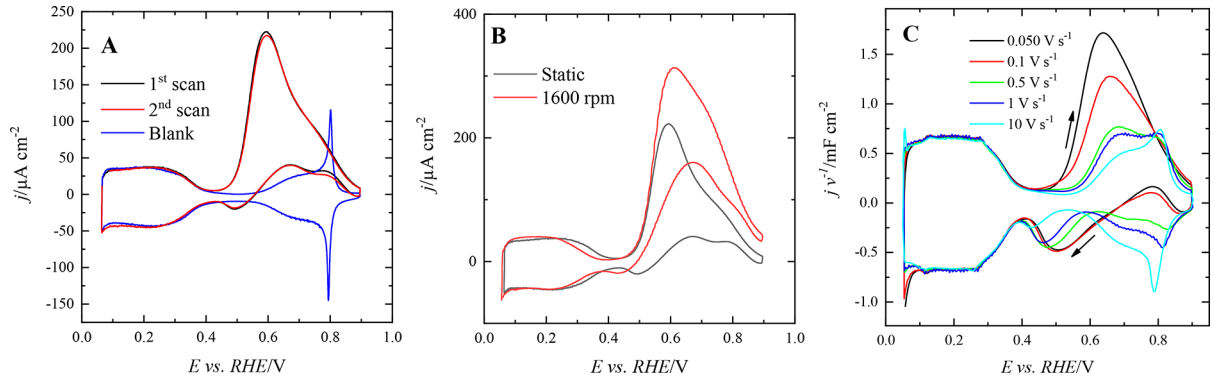

Figure 1. (A) Voltammetric profiles of the Pt(111) electrode in 0.1 M $HClO_4$ in the absence and presence of 1 mM EtOH at 50 mV s^{-1}. (B) Effect of the rotation rate in the voltammetric profiles of the Pt(111) electrode in 0.1 M $HClO_4$ + 1 mM EtOH at 50 mV s^{-1}. (C) Evolution of the voltammetric profile of the Pt(111) (in capacitance units) with scan rate in 0.1 M $HClO_4$ + 0.1 mM EtOH.

participation of additional species playing key roles in these processes.[17] Bidentate adsorbed formate favors the monodentate adsorbed form, which is the active species in the formic acid oxidation reaction,[18] and adsorbed OH is involved in the adsorption of methanol to form adsorbed methoxy in the first step of its oxidation.[19] However, the participation of additional species in the ethanol oxidation reaction has not been established yet.

To better understand the ethanol electro-oxidation mechanism on platinum in acidic media and to determine whether additional adsorbed species are involved in the process, which is essential to optimize catalysts, new experiments on well-defined surfaces (Pt(111) and Pt(100)) and density-functional theory (DFT) calculations are presented herein. Under low ethanol concentrations at different scan rates, oxidation and adsorption processes can be discriminated. Furthermore, using well-defined surfaces, experimental results and calculations can be more confidently correlated. By doing so, the mechanism controlling the selectivity of this reaction and how the C−C bond is cleaved can be elucidated.

METHODS

Experimental Methods. Pt(111) and Pt(100) single-crystal electrodes were prepared from small single-crystal beads (ca. 2.5 mm diameter) obtained by melting a 99.999% purity platinum wire (0.5 mm diameter). These beads were oriented, cut, and polished until mirror finishing using the procedure described by Clavilier.[20] Prior to any experiment, the electrodes were flame annealed, cooled in a H_2/Ar atmosphere, and protected with water in equilibrium with this gas mixture. This procedure leads to well-ordered Pt(111) and Pt(100) surfaces with the nominal orientation.[21] The cleanliness of electrodes and solutions was verified by voltammetry in perchloric acid solutions, and the characteristic voltammetric profiles of the electrodes, which should be stable upon cycling when clean solutions are used, were obtained.

Experiments were carried out at room temperature in classical two-compartment electrochemical cells deaerated using Ar (N50, Air Liquide in all gases used), including a large platinum counter electrode and a reversible hydrogen (N50) electrode (RHE) as the reference. The solutions were prepared using concentrated $HClO_4$ (Merck, for analysis) and ethanol (Merck suprapur). Voltammograms were recorded using an Autolab PGSTAT302N potentiostat in a hanging meniscus configuration. For scan rates higher than 100 mV s^{-1}, the ohmic drop was compensated using the current interruption method.

Computational Methods. All DFT calculations were carried out using numerical basis sets,[22] semicore pseudopotentials[23] (which include scalar relativistic effects), and the RPBE functional[24] as implemented in the Dmol^3 code.[25] Dispersion forces were corrected by the Tkatchenko and Scheffler method.[26] Continuous solvation effects were considered by the COSMO model.[27] Hydrogen bonds were captured by introducing explicit water molecules. The effects of nonzero dipole moments in the supercells were canceled using external fields.[28]

The Pt(111) and Pt(100) surfaces were modeled using a periodic supercell comprised of four layers of metal atoms and a vacuum slab of 20 Å. The bottom two layers were frozen in their bulk crystal locations, whereas the remaining atoms were allowed to relax with the adsorbates. Optimal adsorbent/adsorbate configurations were searched for using numerical basis sets of double-numerical quality. Transition states were searched for using a generalization of the linear synchronous transit method for periodic systems,[29] combined with a quadratic synchronous transit method in a complete protocol as implemented in Dmol^3, and through manual sampling and constrained optimization. The automatically found transition states were confirmed by estimating the minimum energy reaction paths employing the nudged elastic band method.[30] For this phase of the calculations, the optimization convergence thresholds were set to 2.0 × 10^{-5} Ha for the energy, 0.004 Ha/Å for the force, and 0.005 Å for the displacement. The SCF convergence criterion was set to 1.0 × 10^{-5} Ha for the energy. Assuming the previously optimized configurations, energies were estimated using numerical basis sets of double-numerical quality plus polarization. In this case, the SCF convergence criterion was set to 1.0 × 10^{-6} Ha for the energy.

The orbital cutoff radius of 4.5 Å was always used for all of the atoms. Brillouin zones were always sampled, under the Monkhorst−Pack method, using grids corresponding to distances in the reciprocal space on the order of 0.04 1/Å. Convergence was always facilitated by introducing 0.002 Ha of thermal smearing, though the total energies were extrapolated to 0 K. A value of 78.54 was used as the dielectric constant for water in the continuous solvation model.

RESULTS

Experimental Results on Pt(111) and Pt(100). Under usual voltammetric conditions, large oxidation currents mask small currents attributed to adsorption steps, making them difficult to detect such adsorption processes. Low reactant concentrations and/or high scan rates can be used to increase the adsorption currents to oxidation currents ratio so that the adsorbed species can be easily detected. These strategies have already revealed the roles played by adsorbed formate in the formic acid oxidation[31] and by adsorbed OH in the methanol oxidation reaction.[19] These approaches have been also used in this research to investigate the adsorption processes involved in ethanol oxidation on platinum in aqueous electrolytes. From the comparison between the voltammetric profiles obtained in the absence and the presence of 1 mM ethanol for the Pt(111)

https://doi.org/10.1021/acssuschemeng.2c02663
ACS Sustainable Chem. Eng. 2023, 11, 4960−4968

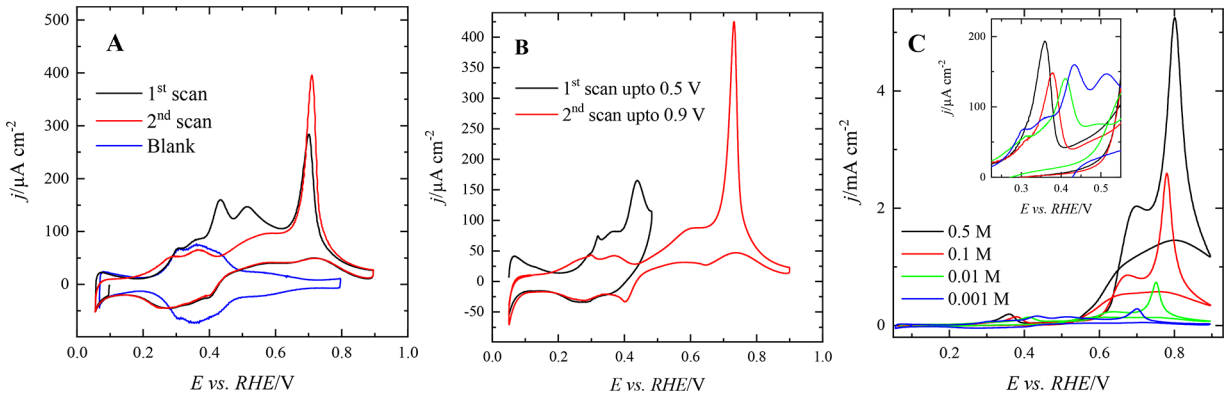

Figure 2. (A) Voltammetric profiles of the Pt(100) electrode in 0.1 M $HClO_4$ in the absence (blue line) and presence of 1 mM EtOH (black line, first scan; red line, second scan) at 50 mV s^{-1}. (B) Effect of the upper potential limit in the voltammetric profiles of the Pt(100) electrode in 0.1 M $HClO_4$ + 1 mM EtOH at 50 mV s^{-1}. (C) Effect of the ethanol concentration in the voltammetric profile of the Pt(100) in 0.1 M $HClO_4$ at 50 mV s^{-1}.

electrode (Figure 1A), three pieces of evidence regarding the adsorption processes on this surface can be obtained. First, the onset of the ethanol oxidation reaction is ca. 0.45 V, which is lower than that obtained for methanol oxidation.[19] To establish whether the ethanol oxidation reaction is triggered by the presence of adsorbed OH on the surface, the onset of OH adsorption has to be determined. It is generally accepted that OH adsorption takes place at potentials higher than 0.55 V because from that point currents start to increase. However, the actual onset for OH adsorption is lower. Although the currents measured in the region between 0.4 and 0.55 V are mainly due to the double-layer charging processes, OH adsorption can also contribute to them. To separate both contributions, the current for the double-layer processes calculated by thermodynamic analysis in perchloric acid solutions will be used.[32] As shown in Figure S1, experimental currents are higher than those calculated for the double-layer process for E > 0.45 V. The excess of the measured current then must be assigned to the OH adsorption process, and consequently, the onset for OH adsorption is 0.45 V. It should be noted that the potential of zero free charge (pzfc) for this surface is located at 0.34 V vs RHE,[33] and thus, from that potential, the surface charge is positive, which favors the adsorption of OH. Therefore, the onset of the ethanol oxidation reaction is linked to the onset of OH adsorption. The higher reactivity for the ethanol oxidation reaction on this surface[13] versus that of methanol[34] explains the lower onset for the ethanol oxidation reaction. For methanol oxidation, it was found that adsorbed OH favors the adsorption and conversion of methanol into adsorbed methoxy.[19] Thus, a similar role for adsorbed OH can be anticipated in the adsorption and conversion of ethanol into adsorbed ethoxy. Second, given that no differences can be observed in the hydrogen adsorption region (from 0.05 to 0.4 V) between the first and the second scan, it can be concluded that adsorbed CO is not being accumulated during this electro-oxidation process.[13] Third, currents in the negative scan direction significantly smaller than those in the positive scan direction clearly indicate oxidation inhibition by the presence of adsorbate. This inhibition can be attributed to acetic acid adsorbed as acetate,[13] which has been detected by FTIR and ATR-SEIRAS at these potential values.[16,35] Acetate formation is probably independent of the acetaldehyde formation since no acetate was detected previously by Rodriguez et al. during the acetaldehyde oxidation on Pt(111) and Pt(100) by FTIR.[36] Indeed, Giz et al. found that the onset for acetic acid formation on Pt(111) takes place at lower potentials than the formation of acetaldehyde, which suggests that the production of acetic acid may follow a parallel pathway that does not have acetaldehyde as an intermediate.[37]

The acetate inhibition effect can be further corroborated using a rotating disk configuration. For the conditions of Figure 1A, no effect of the rotation rate on the measured currents would have been expected because these are well below the limiting diffusion current of ethanol for this concentration (ca. 6−8 mA cm^{-2}). However, a significant current increase is observed at 1600 rpm, especially in the negative scan direction (Figure 1B). This current increase can be attributed to the lower interfacial concentration of acetic acid convectively removed from the interface, which leads to a lower acetate coverage and a lower oxidation inhibition.

To discard the participation of adsorbed species other than OH and acetate, voltammetric profiles for the Pt(111) electrode in 0.1 M $HClO_4$ + 0.1 mM EtOH at different scan rates were recorded (Figure 1C). At this low concentration, the acetate desorption signal can be observed in the negative scan direction as a broad peak centered at ca. 0.5 V. This signal diminishes with increasing scan rate, disappearing at 10 V s^{-1} and giving rise to a voltammogram that is identical to the one recorded at this scan rate in the absence of ethanol. Thus, it can be concluded that no other adsorbed species can be detected during this oxidation and that the presence of ethanol in the solution does not alter the OH adsorption profile.

Acetate may directly hinder the reaction by preventing the interaction of ethanol with the surface, but it may also indirectly displace adsorbates required in this process. Adsorbed acetate on Pt(111) forms a relaxed adlayer with relatively low coverage (ca. 0.2) participated by water.[38] The presence of this acetate layer does not inhibit formic acid oxidation on this surface, implying that the nature of the acetate adlayer does not hinder the interaction of formic acid with the substrate.[39] However, acetate prevents OH adsorption on Pt(111), giving rise to significantly lower currents for reactions in which this species is involved as a reactant, as happens, for instance, in methanol oxidation.[40] In this sense, Giz et al. found an increasing difficulty to oxidize CO generated on the possible defects present on a Pt(111) surface by increasing the ethanol concentration, attributed to the

https://doi.org/10.1021/acssuschemeng.2c02663
ACS Sustainable Chem. Eng. 2023, 11, 4960−4968

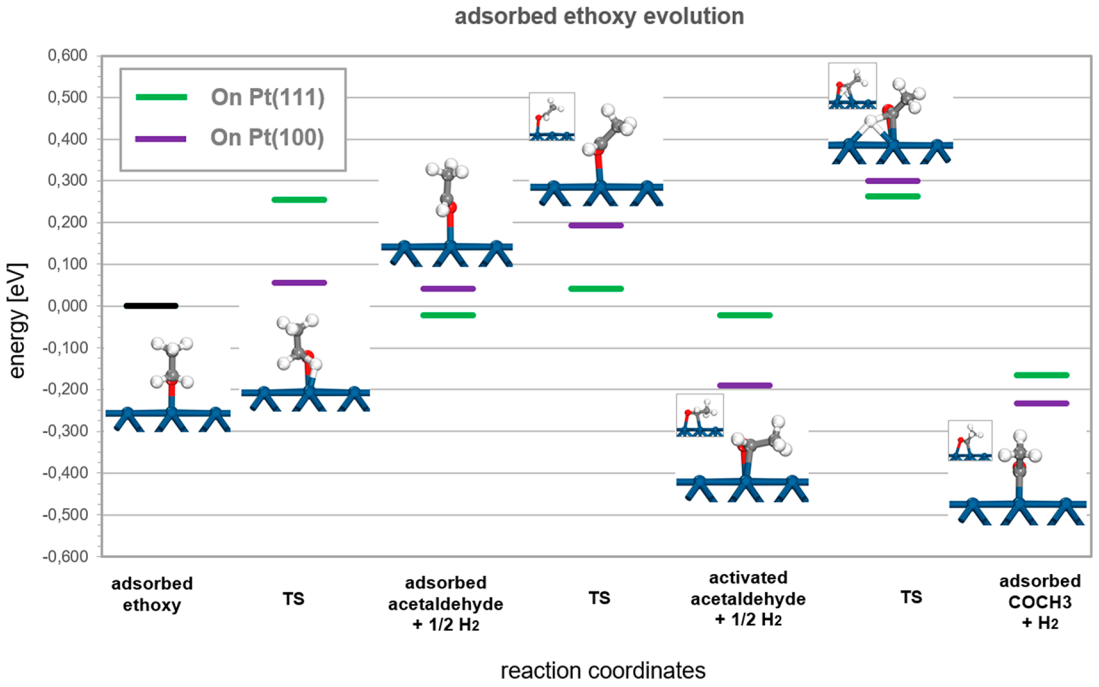

Figure 3. Energy profiles for the adsorbed ethoxy evolution to adsorbed $COCH_3$ on Pt(111) and Pt(100). Being similar on Pt(111), reactant, intermediates, transition states, and products are displayed only on Pt(100).

blockage of the Pt surface by intermediates (possibly acetate) that inhibits the OH adsorption.[37] The comparison between the formic acid oxidation behavior on one side and those of methanol and ethanol on the other further reinforces the conclusion that adsorbed OH plays an essential role in the ethanol oxidation reaction on platinum electrodes.

Similar experiments were conducted on Pt(100). In the voltammetric profiles obtained in the absence and presence of 1 mM ethanol for this electrode (Figure 2A), it can be observed that during the first scan these profiles are identical up to 0.35 V. Then, additional peaks appear at ca. 0.42, 0.5, and 0.7 V in the presence of ethanol. This latter peak can be assigned to adsorbed CO oxidation, which is formed when breaking the C−C bond of ethanol on the surface.[13] In the negative scan direction, currents are very low and the hydrogen profile recorded between 0.3 and 0.06 V is partially blocked, indicating that CO has been already formed. In the second and subsequent scans, the peaks at 0.42 and 0.5 V are not observed and the peak related to the oxidation of CO is larger. The absence of the peaks at 0.42 and 0.5 V in the second scan suggests that they are connected to an oxidative adsorption process. Apart from the CO oxidation peak, the measured currents for Pt(100) are significantly smaller than those recorded on Pt(111).

To gain insight into the nature of the oxidative adsorption process on Pt(100), a freshly annealed electrode was immersed, reversing the scan after the peak at 0.42 V (Figure 2B). In the negative scan direction, the hydrogen profile is partially blocked, being clear proof of the formation of an irreversibly adsorbed species. Furthermore, in the subsequent positive scan direction, no peak is observed between 0.4 and 0.6 V and the peak at 0.7 V is larger. Although the peak at 0.42 V is always present under different concentrations (Figure 2C), shifting to lower values as the concentration increases, the charge under this peak remains almost constant, which confirms its relationship with the formation of an adsorbed species from ethanol.

All of these results indicate that the peaks at 0.42 and 0.5 V are related to the formation of adsorbed CO from the C−C bond cleavage of ethanol on Pt(100). In fact, the peak at 0.42 V is very similar to that observed for methanol oxidation, which has been attributed to the formation of adsorbed CO.[41] Finally, it should be noticed that the onset for cleavage of the C−C bond, leading to formation of adsorbed CO, coincides with that of the OH adsorption on this electrode (ca. 0.35 V), which reveals that both processes are connected, that is, adsorbed OH is required to activate and completely oxidize ethanol on Pt(100).

In summary, as recently found for methanol,[19] the ethanol electro-oxidation on platinum in water, both on Pt(111) and on Pt(100), takes place only in the presence of adsorbed OH. Large oxidation currents were measured on Pt(111), although CO was not detected during the process. This fact implies that ethanol is not being completely oxidized on Pt(111). By contrast, less intense oxidation currents were measured on Pt(100), although CO was formed in this case. This observation implies that the ethanol C−C bond is being cleaved on Pt(100). From these key experimental findings and DFT calculations, the mechanisms controlling the ethanol electro-oxidation selectivity on platinum in water as a model system can be elucidated.

Activation Mechanism. It has been recently shown that the coadsorption of OH and methanol in neighboring locations favors methanol activation on platinum in water, giving rise to adsorbed methoxy and water in a virtually barrierless step.[19] Since ethanol and methanol have similar adsorption modes and their oxidation processes take place only in the presence of adsorbed OH, the activation mechanism found for methanol was also tested for ethanol. The observed mechanism is almost identical with that observed for methanol, that is, adsorbed OH plays a key role as a reactant in this

https://doi.org/10.1021/acssuschemeng.2c02663
ACS Sustainable Chem. Eng. 2023, 11, 4960−4968

mechanism, which is facilitating the formation of adsorbed ethoxy. The availability of this key reactant at the right location for the reaction (close to an adsorbed ethanol molecule) is controlled by the adsorbate/media/surface interactions in the interface. The nearly perfect match between the geometry of the water lattice at the interface and the specific atomic arrangement of the Pt(111) surface[42] (hexagonal lattices with almost identical parameters) allows for optimal oxygen/platinum interactions on top locations while maintaining the network of hydrogen bonds. The congruence of the lattices leads to a quasi-negligible hydrogen transfer barrier between adjacent oxygen atoms in the water layer, ensuring the fast movement of adsorbed OH on this plane toward the right location. Conversely, the larger mismatch between the water lattice at the interface and the specific atomic arrangement of the Pt(100)[43] surface (hexagonal vs square lattices) forces the competition between hydrogen bonds and optimal oxygen/platinum interactions on top locations, giving rise to a more sluggish dynamic evolution of adsorbed OH on this plane. This mechanism can explain a faster ethanol activation rate on Pt(111), resulting in higher ethanol oxidation currents on this surface in agreement with the experimental findings.

Evolution to Adsorbed $COCH_3$. To explore the adsorbed ethoxy evolution to adsorbed $COCH_3$ on Pt(111) and Pt(100), DFT calculations on periodic models of these surfaces were carried out. It was found that adsorbed ethoxy can readily evolve to adsorbed $COCH_3$, both on Pt(111) and on Pt(100), according to the mechanism schematized in the energy profiles of Figure 3. Adsorbed ethoxy can favorably yield adsorbed acetaldehyde, which then can be easily activated and dehydrogenated to give rise to adsorbed $COCH_3$. The successive bonding mode switching of the C−O bond along this process, from a single to a double bond (to yield acetaldehyde) and then to single bond (to activate acetaldehyde) and once more time to a double bond (to give rise to adsorbed $COCH_3$) enables the smooth transition between intermediates, providing easily accessible bonding alternatives.

Acetic Acid Formation. After verifying that the involved coadsorptions are not repulsive, acetic acid formation was computationally investigated on Pt(111) and Pt(100) from the configurations shown in Figure 4. A continuous solvation model was only used initially as a solvation effect treatment. Although this reaction is clearly favorable by more than 1 eV on Pt(111) and only slightly favorable on Pt(100) by ca. 0.1 eV, the calculations indicate that acetic acid can be much more readily formed on Pt(111) than on Pt(100) because of the difference in the barriers (no barrier on Pt(111) vs 0.67 eV on Pt(100)). This preliminary conclusion partially explains why ethanol is not completely oxidized on Pt(111). Three reasons can be pointed out to explain this large barrier difference between both surfaces. First, in the involved reactant configurations (Figure 4), adsorbed OH is much closer to the target carbon on Pt(111) than that on Pt(100) (2.62 vs 3.13 Å). Second, OH is much more intensely adsorbed on the bridge-bond location on Pt(100) (the initial position of this reactant for this reaction step on this surface) than on the on-top location on Pt(111) (by 0.78 eV). Third, the OH group maintains a more favorable orientation along the reaction path on Pt(111) than on Pt(100). Alternative configurations for this step on Pt(100) were also studied (Figure S2), although the calculated barrier was higher.

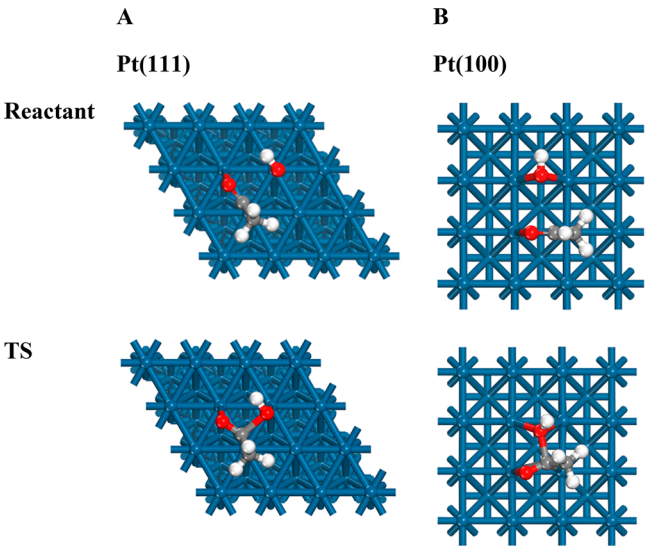

Figure 4. Reactant and transition state configurations for the incorporation reaction of adsorbed OH to the adsorbed $COCH_3$ intermediate to yield acetic acid on (A) Pt(111) and (B) Pt(100).

Solvation Effects. Additional interfacial solvation effects involved in the acetic acid formation step from the adsorbed $COCH_3$ intermediate on Pt(111) were investigated by including explicit water molecules in the models (Figure 5).

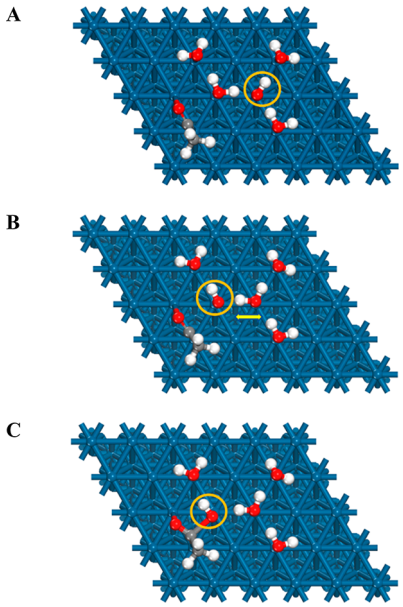

Figure 5. Relevant configurations used to study in detail the solvation effect involved in the incorporation reaction of adsorbed OH to the adsorbed $COCH_3$ intermediate to yield acetic acid on Pt(111): (A) reactant, (B) pseudostate defined by the optimization constraint indicated in the figure, and (C) transition state. Orange circles highlight the adsorbed OH evolution. Yellow arrow represents an optimization constraint.

It was found that OH is not stable in the adjacent location to the intermediate since adsorbed OH is more favorably solvated inside the water network at the interface. Thus, the configuration displayed in Figure 5A has to be considered as the reference reactant state for this reaction step. This result contrasts with recent findings for methanol, where the

https://doi.org/10.1021/acssuschemeng.2c02663
ACS Sustainable Chem. Eng. 2023, 11, 4960−4968

coadsorption of methanol by the OH group and OH in adjacent locations is favored by hydrogen-bond formation.[19] From this reactant state, the reaction barrier to form acetic acid on Pt(111), corresponding to the transition state of Figure 5C, was found to be 0.36 eV. This significant barrier (vs no barrier under continuum solvation conditions only) can be explained by two effects. First, adsorbed OH has to be extracted from inside the water lattice in the interface, where it possesses higher solvation energy, to the edge of this lattice, where it can take part in the reaction step. Second, the interaction between adsorbed OH and the water lattice has to be weakened in the transition state to eventually yield acetic acid in a very favorable reaction step. In any case, the reaction rate for this step strongly depends on the adsorbed OH diffusion rate, which controls the movement of adsorbed OH toward the reacting site. To better understand the kinetic aspects of this reaction step, the pseudostate in Figure 5B, obtained constraining the indicated OH bond to a typical value of this kind of bond in a water lattice in this interface, was considered. Since the barrier to this reaction step on Pt(111) is essentially zero in the absence of solvation effects associated with hydrogen bonds, consideration of this pseudostate allows decomposing the estimated barrier of 0.36 eV into two contributions: one for each of the two aforementioned effects. It was found that this pseudostate (Figure 5B) is unfavorably reached from the reactant state (Figure 5A) by only 0.15 eV. Furthermore, the fast dynamics of adsorbed OH on Pt(111) guarantee the frequent availability of this reactant in the reactive location, maximizing the viability of this reaction step. Thus, it can be confirmed that acetic acid formation is a facile reaction on Pt(111) with a total barrier of only 0.36 eV after considering interfacial solvation effects. However, although this mechanism explains why acetic acid is readily formed on Pt(111), it does not justify why ethanol is not completely oxidized on this surface.

A similar evaluation of the role played by the interfacial solvation effects on the acetic acid formation reaction on Pt(100) would be desirable. However, the configurations for adsorbed OH and water on Pt(100) are much more complex.[44] For this reason, interfacial solvation effects on Pt(100) for this reaction step were estimated from the analysis performed on Pt(111). Since adsorbed OH would be solvated worse on Pt(100), the energy involved in the movement of adsorbed OH from inside the water lattice to the edge on this surface should be lower and might range between one-half and two-thirds of that calculated on Pt(111). Furthermore, since only one hydrogen bond with the water lattice is broken to form the transition state on Pt(100) instead of two on Pt(111), this energetic component should be also reduced to one-half. Thus, the barrier to the acetic acid formation on Pt(100) should be, at least, on the order of 0.85 eV. This high barrier confirms that acetic acid cannot be so readily formed on Pt(100) as it can be formed on Pt(111), although it does not explain how ethanol is completely oxidized on Pt(100).

CH_3 Group Activation. To completely understand why ethanol cannot be completely oxidized on Pt(111), the CH_3 group activation from the adsorbed $COCH_3$ intermediate to form adsorbed $COCH_2$ was investigated on Pt(111) as an alternative step to the formation of acetic acid. This activation is the first step in breaking the C−C bond, leading to complete oxidation of the fuel. Although mechanisms in the presence and absence of adsorbed OH were explored, direct involvement of adsorbed OH in this reaction step was not observed. Thus, the energy profile for this step was estimated from the transition state of Figure 6A (the whole step is presented in Figure S3A). It was found that dehydrogenation of the CH_3 group on Pt(111) to yield adsorbed CH_2CO is slightly unfavorable by 0.14 eV with a barrier of 0.86 eV. A significant rate for the C−C bond cleavage requires, at least, that the barrier for CH_3 group dehydrogenation was comparable to that calculated for the acetic acid formation. Thus, despite ethanol electro-oxidation selectivity being frequently analyzed focusing on the C−C bond cleavage step, the real reason ethanol is not completely oxidized on Pt(111) is not that the C−C bond cleavage is impeded but rather that the step leading to acetic acid formation is much more favorable than CH_3 group activation on this surface.

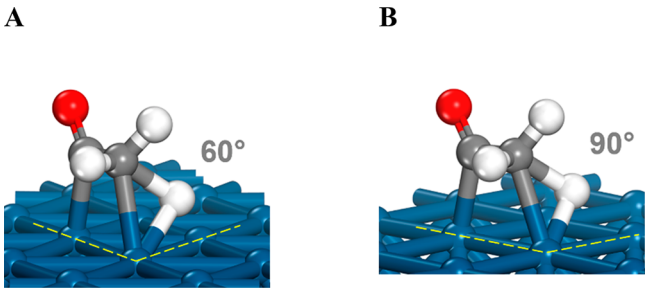

Figure 6. Transition states corresponding to the CH_3 group from the $COCH_3$ intermediate activation reactions on (A) Pt(111) and (B) Pt(100) are completely schematized in Figure S3.

To achieve CH_3 group activation (a necessary step for complete oxidation of the fuel), the availability of adsorbed OH, the barrier for the acetic acid formation, and/or the CH_3 group activation barrier should be diminished. All three mechanisms simultaneously operate on Pt(100). As aforementioned, much more sluggish dynamics for adsorbed OH can be expected on Pt(100). A higher barrier to acetic acid formation (0.85 vs 0.36 eV) was found on Pt(100). Finally, a much more accessible CH_3 group activation step (0.55 vs 0.86 eV as a barrier, for a similar total energy) was found on Pt(100) (Figures 6B and S3B). Thus, the significantly lower barrier for CH_3 group activation than that for acetic acid formation allows for complete ethanol oxidation on Pt(100).

The CH_3 group dehydrogenation barriers on platinum on Pt(111) and Pt(100) are not small because, as can be observed in Figure 6, the C−H bond has to be extraordinarily elongated (from ca. 1.10 to ca. 1.60 Å) on both electrodes before the carbon and hydrogen atoms can simultaneously interact with platinum to give rise to the dehydrogenation step. The barrier on Pt(100) is smaller than that on Pt(111) (0.55 vs 0.86 eV) since the broader output angle for hydrogen on Pt(100) (90° vs 60°) avoids repulsion between the dehydrogenated fragment and the hydrogen atom (Figure 5).

C−C Bond Cleavage. The ethanol C−C bond can be favorably cleaved from the $COCH_2$ intermediate (by 0.27 eV with a barrier of 0.81 eV) on Pt(100) according to the reaction step schematized in Figure 7. The alternative mechanism under which the CH_2 group is displaced in the opposite direction was also considered (Figure S4), although it was found to be less favorable.

https://doi.org/10.1021/acssuschemeng.2c02663
ACS Sustainable Chem. Eng. 2023, 11, 4960−4968

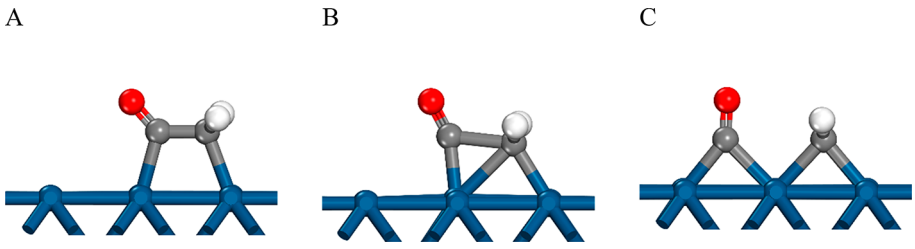

Figure 7. Ethanol C−C bond cleavage mechanism from the $COCH_2$ intermediate to yield adsorbed CO and adsorbed CH_2 on Pt(100): (A) reactant, (B) transition state, and (C) product.

CONCLUSIONS

The practical utility of the fuel cell approach to obtain as much of the energy stored in ethanol as possible depends on the availability of catalysts with enough selectivity toward complete electro-oxidation of this fuel. The reported experimental results provide evidence that the ethanol electro-oxidation on platinum in aqueous media takes place only in the presence of adsorbed OH. Ethanol can be not completely oxidized on Pt(111), whereas adsorbed CO is readily formed on Pt(100). The participation of adsorbed OH as a reactant in the mechanism explains why a large oxidation inhibition is observed when acetic acid is formed resulting in acetate adsorption. Although the acetate layer allows ethanol/surface interaction, it hinders OH adsorption, which is a required species in this oxidation mechanism. Computational results confirm the participation of adsorbed OH in this process, providing a detailed mechanism. Adsorbed OH is required to form adsorbed ethoxy, which then evolves to adsorbed $COCH_3$. From this intermediate, the calculated barriers for the different steps in the oxidation mechanism are very dependent on the surface structure, which explains the experimental differences observed for this oxidation process on Pt(111) and Pt(100). Adsorbed $COCH_3$ readily reacts with an additional adsorbed OH species to yield acetic acid on Pt(111). By contrast, the higher barrier for this step enables the dehydrogenation of the CH_3 group to yield adsorbed CH_2CO on Pt(100). From this latter species, the C−C bond can be favorably cleaved on Pt(100). The evolution dynamics of adsorbed OH on the surface, which depends on the adsorbate/media/surface interactions at the interface, modulate the availability of this key reactant, controlling the kinetics of the reaction. It has been also shown that the involvement of adsorbed OH in the water lattice at the interface can have a significant impact on the estimation of barriers for the reaction steps in which adsorbed OH takes part as a reactant. The experimental and computational results are therefore mutually consistent. Furthermore, the feasibility of each reaction step has been discussed in terms of fundamental effects and mechanisms. Thus, not only the C−C bond cleavage but also the CH_3 group activation from the adsorbed $COCH_3$ intermediate should be considered when analyzing the selectivity of the ethanol oxidation reaction. In fact, these results explain the observed behavior of the reaction on platinum electrodes modified by oxophilic elements, such as tin. Although effective catalysis is observed, the selectivity for CO_2 is not improved[12,45] because the increased availability of adsorbed OH on the surface due to the presence of tin promotes the incomplete oxidation of ethanol. These insights can contribute to accelerating the development of selective catalysts for this fuel and to a better understanding of the oxidation reactions of alcohols on platinum in aqueous media and other reactions in which adsorbed OH plays a key role as a reactant. Moreover, this manuscript provides evidence that electrocatalytic selectivity research requires holistic consideration of the reactants, adsorbates, media, and substrate in a potential-dependent environment.

ASSOCIATED CONTENT

Supporting Information

The Supporting Information is available free of charge at https://pubs.acs.org/doi/10.1021/acssuschemeng.2c02663.

Additional figures for the calculations (PDF)

AUTHOR INFORMATION

Corresponding Authors

Adolfo Ferre-Vilaplana − *Instituto Tecnológico de Informática, Ciudad Politécnica de la Innovación, Valencia E-46022, Spain; Departamento de Sistemas Informáticos y Computación, Escuela Politécnica Superior de Alcoy, Universidad Politécnica de Valencia, Alcoy E-03801, Spain;* orcid.org/0000-0002-9032-9015; Email: aferre@dsic.upv.es

Enrique Herrero − *Instituto de Electroquímica, Universidad de Alicante, Alicante E-03080, Spain;* orcid.org/0000-0002-4509-9716; Email: herrero@ua.es

Authors

Rubén Rizo − *Instituto de Electroquímica, Universidad de Alicante, Alicante E-03080, Spain;* orcid.org/0000-0001-8161-2989

Juan M. Feliu − *Instituto de Electroquímica, Universidad de Alicante, Alicante E-03080, Spain;* orcid.org/0000-0003-4751-3279

Complete contact information is available at: https://pubs.acs.org/10.1021/acssuschemeng.2c02663

Author Contributions

The manuscript was written through the contributions of all authors. All authors have approved the final version of the manuscript.

Notes

The authors declare no competing financial interest.

ACKNOWLEDGMENTS

This research was funded by Ministerio de Ciencia e Innovación (Spain) grant nos. PID2019-105653GB-I00 and FJC2018-038607-I and Generalitat Valenciana (Spain) grant no. PROMETEO/2020/063.

REFERENCES

(1) Zhong, M.; Tran, K.; Min, Y.; Wang, C.; Wang, Z.; Dinh, C. T.; De Luna, P.; Yu, Z.; Rasouli, A. S.; Brodersen, P.; Sun, S.; Voznyy, O.; Tan, C. S.; Askerka, M.; Che, F.; Liu, M.; Seifitokaldani, A.; Pang, Y.; Lo, S. C.; Ip, A.; Ulissi, Z.; Sargent, E. H. Accelerated Discovery of CO2 Electrocatalysts Using Active Machine Learning. *Nature* **2020**, *581* (7807), 178−183.

(2) Peters, I. M.; Breyer, C.; Jaffer, S. A.; Kurtz, S.; Reindl, T.; Sinton, R.; Vetter, M. The Role of Batteries in Meeting the PV Terawatt Challenge. *Joule* **2021**, *5* (6), 1353−1370.

(3) Kempler, P. A.; Slack, J. J.; Baker, A. M. Research Priorities for Seasonal Energy Storage Using Electrolyzers and Fuel Cells. *Joule* **2022**, *6* (2), 280−285.

(4) Lin, H.; Luo, S.; Zhang, H.; Ye, J. Toward Solar-Driven Carbon Recycling. *Joule* **2022**, *6* (2), 294−314.

(5) Pellow, M. A.; Emmott, C. J. M.; Barnhart, C. J.; Benson, S. M. Hydrogen or Batteries for Grid Storage? A Net Energy Analysis. *Energy Environ. Sci.* **2015**, *8* (7), 1938−1952.

(6) Manochio, C.; Andrade, B. R.; Rodriguez, R. P.; Moraes, B. S. Ethanol from Biomass: A Comparative Overview. *Renew. Sustain. Energy Rev.* **2017**, *80*, 743−755.

(7) Birdja, Y. Y.; Pérez-Gallent, E.; Figueiredo, M. C.; Göttle, A. J.; Calle-Vallejo, F.; Koper, M. T. M. Advances and Challenges in Understanding the Electrocatalytic Conversion of Carbon Dioxide to Fuels. *Nat. Energy* **2019**, *4* (9), 732−745.

(8) An, B.; Li, Z.; Song, Y.; Zhang, J.; Zeng, L.; Wang, C.; Lin, W. Cooperative Copper Centres in a Metal−Organic Framework for Selective Conversion of CO2 to Ethanol. *Nat. Catal.* **2019**, *2* (8), 709−717.

(9) Wang, X.; Wang, Z.; García de Arquer, F. P.; Dinh, C. T.; Ozden, A.; Li, Y. C.; Nam, D. H.; Li, J.; Liu, Y. S.; Wicks, J.; Chen, Z.; Chi, M.; Chen, B.; Wang, Y.; Tam, J.; Howe, J. Y.; Proppe, A.; Todorović, P.; Li, F.; Zhuang, T. T.; Gabardo, C. M.; Kirmani, A. R.; McCallum, C.; Hung, S. F.; Lum, Y.; Luo, M.; Min, Y.; Xu, A.; O'Brien, C. P.; Stephen, B.; Sun, B.; Ip, A. H.; Richter, L. J.; Kelley, S. O.; Sinton, D.; Sargent, E. H. Efficient Electrically Powered CO2-to-Ethanol via Suppression of Deoxygenation. *Nat. Energy* **2020**, *5* (6), 478−486.

(10) Xu, H.; Rebollar, D.; He, H.; Chong, L.; Liu, Y.; Liu, C.; Sun, C. J.; Li, T.; Muntean, J. V.; Winans, R. E.; Liu, D. J.; Xu, T. Highly Selective Electrocatalytic CO2 Reduction to Ethanol by Metallic Clusters Dynamically Formed from Atomically Dispersed Copper. *Nat. Energy* **2020**, *5* (8), 623−632.

(11) Rizo, R.; Pérez-Rodríguez, S.; García, G. Well-Defined Platinum Surfaces for the Ethanol Oxidation Reaction. *ChemElectroChem.* **2019**, *6* (18), 4725−4738.

(12) Wang, Q.; Sun, G. Q.; Jiang, L. H.; Xin, Q.; Sun, S. G.; Jiang, Y. X.; Chen, S. P.; Jusys, Z.; Behm, R. J. Adsorption and Oxidation of Ethanol on Colloid-Based Pt/C, PtRu/C and Pt3Sn/C Catalysts: In Situ FTIR Spectroscopy and on-Line DEMS Studies. *Phys. Chem. Chem. Phys.* **2007**, *9* (21), 2686−2696.

(13) Colmati, F.; Tremiliosi-Filho, G.; Gonzalez, E. R. E. R.; Berná, A.; Herrero, E.; Feliu, J. M. J. M. Surface Structure Effects on the Electrochemical Oxidation of Ethanol on Platinum Single Crystal Electrodes. *Faraday Discuss.* **2009**, *140*, 379−397.

(14) Colmati, F.; Tremiliosi-Filho, G.; Gonzalez, E. R.; Berna, A.; Herrero, E.; Feliu, J. M. The Role of the Steps in the Cleavage of the C-C Bond during Ethanol Oxidation on Platinum Electrodes. *Phys. Chem. Chem. Phys.* **2009**, *11* (40), 9114−9123.

(15) Ferre-Vilaplana, A.; Buso-Rogero, C.; Feliu, J. M.; Herrero, E. Cleavage of the C-C Bond in the Ethanol Oxidation Reaction on Platinum. Insight from Experiments and Calculations. *J. Phys. Chem. C* **2016**, *120* (21), 11590−11597.

(16) Rodes, A.; Pastor, E.; Iwasita, T. An Ftir Study on the Adsorption of Acetate at the Basal Planes of Platinum Single-Crystal Electrodes. *J. Electroanal. Chem.* **1994**, *376* (1−2), 109−118.

(17) Rizo, R.; Arán-Ais, R. M.; Herrero, E. On the Oxidation Mechanism of C1-C2 Organic Molecules on Platinum. A Comparative Analysis. *Curr. Opin. Electrochem.* **2021**, *25*, 100648.

(18) Ferre-Vilaplana, A.; Perales-Rondón, J. V. V.; Buso-Rogero, C.; Feliu, J. M. M.; Herrero, E. Formic Acid Oxidation on Platinum Electrodes: A Detailed Mechanism Supported by Experiments and Calculations on Well-Defined Surfaces. *J. Mater. Chem. A* **2017**, *5* (41), 21773−21784.

(19) Mekazni, D. S.; Arán-Ais, R. M.; Ferre-Vilaplana, A.; Herrero, E. Why Methanol Electro-Oxidation on Platinum in Water Takes Place Only in the Presence of Adsorbed OH. *ACS Catal.* **2022**, *12* (3), 1965−1970.

(20) Clavilier, J.; Faure, R.; Guinet, G.; Durand, R. Preparation of Monocrystalline Pt Microelectrodes and Electrochemical Study of the Plane Surfaces Cut in the Direction of the {111} and {110} Planes. *J. Electroanal. Chem.* **1980**, *107* (1), 205−209.

(21) Herrero, E.; Orts, J. M.; Aldaz, A.; Feliu, J. M. Scanning Tunneling Microscopy and Electrochemical Study of the Surface Structure of Pt(10,10,9) and Pt(11,10,10) Electrodes Prepared under Different Cooling Conditions. *Surf. Sci.* **1999**, *440* (1−2), 259−270.

(22) Delley, B. An Allelectron Numerical Method for Solving the Local Density Functional for Polyatomic Molecules An All-Electron Numerical Method for Solving the Local Density Functional for Polyatomic Molecules. *J. Chem. Phys.* **1990**, *92* (1), 508−517.

(23) Delley, B. Hardness Conserving Semilocal Pseudopotentials. *Phys. Rev. B* **2002**, *66* (15), 155125.

(24) Hammer, B.; Hansen, L. B.; Nørskov, J. K. Improved Adsorption Energetics within Density-Functional Theory Using Revised Perdew-Burke-Ernzerhof Functionals. *Phys. Rev. B* **1999**, *59* (11), 7413−7421.

(25) Delley, B. From Molecules to Solids with the DMol(3) Approach. *J. Chem. Phys.* **2000**, *113* (18), 7756−7764.

(26) Tkatchenko, A.; Scheffler, M. Accurate Molecular Van Der Waals Interactions from Ground-State Electron Density and Free-Atom Reference Data. *Phys. Rev. Lett.* **2009**, *102* (7), 73005.

(27) Delley, B. The Conductor-like Screening Model for Polymers and Surfaces. *Mol. Simul.* **2006**, *32* (2), 117−123.

(28) Neugebauer, J.; Scheffler, M. Adsorbate-Substrate and Adsorbate-Adsorbate Interactions of Na and K Adlayers on Al(111). *Phys. Rev. B* **1992**, *46* (24), 16067−16080.

(29) Halgren, T. A.; Lipscomb, W. N. The Synchronous-Transit Method for Determining Reaction Pathways and Locating Molecular Transition States. *Chem. Phys. Lett.* **1977**, *49* (2), 225−232.

(30) Henkelman, G.; Jónsson, H. Improved Tangent Estimate in the Nudged Elastic Band Method for Finding Minimum Energy Paths and Saddle Points. *J. Chem. Phys.* **2000**, *113* (22), 9978−9985.

(31) Grozovski, V.; Vidal-Iglesias, F. J.; Herrero, E.; Feliu, J. M. Adsorption of Formate and Its Role as Intermediate in Formic Acid Oxidation on Platinum Electrodes. *ChemPhysChem* **2011**, *12* (9), 1641−1644.

(32) Garcia-Araez, N.; Climent, V.; Herrero, E.; Feliu, J. M. M.; Lipkowski, J. Thermodynamic Approach to the Double Layer Capacity of a Pt(1 1 1) Electrode in Perchloric Acid Solutions. *Electrochim. Acta* **2006**, *51* (18), 3787−3793.

(33) Rizo, R.; Sitta, E.; Herrero, E.; Climent, V.; Feliu, J. M. J. M. Towards the Understanding of the Interfacial PH Scale at Pt(111) Electrodes. *Electrochim. Acta* **2015**, *162* (0), 138−145.

(34) Grozovski, V.; Climent, V.; Herrero, E.; Feliu, J. M. The Role of the Surface Structure in the Oxidation Mechanism of Methanol. *J. Electroanal. Chem.* **2011**, *662* (1), 43−51.

(35) Shao, M. H.; Adzic, R. R. Electrooxidation of Ethanol on a Pt Electrode in Acid Solutions: In Situ ATR-SEIRAS Study. *Electrochim. Acta* **2005**, *50* (12), 2415−2422.

(36) Rodriguez, J. L.; Pastor, E.; Xia, X. H.; Iwasita, T. Reaction Intermediates of Acetaldehyde Oxidation on Pt(111) and Pt(100). An in Situ FTIR Study. *Langmuir* **2000**, *16* (12), 5479−5486.

(37) Giz, M. J.; Camara, G. A. The Ethanol Electrooxidation Reaction at Pt (1 1 1): The Effect of Ethanol Concentration. *J. Electroanal. Chem.* **2009**, *625* (2), 117−122.

(38) Zuo, X. Q.; Chen, W.; Yu, A.; Le Xu, M.; Cai, J.; Chen, Y.-X. PH Effect on Acetate Adsorption at Pt(111) Electrode. *Electrochem. commun.* **2018**, *89*, 6−9.

https://doi.org/10.1021/acssuschemeng.2c02663
ACS Sustainable Chem. Eng. 2023, 11, 4960−4968

(39) Perales-Rondón, J. V.; Herrero, E.; Feliu, J. M. Effects of the Anion Adsorption and PH on the Formic Acid Oxidation Reaction on Pt(111) Electrodes. *Electrochim. Acta* **2014**, *140*, 511−517.
(40) Herrero, E.; Franaszczuk, K.; Wieckowski, A. Electrochemistry of Methanol at Low Index Crystal Planes of Platinum. An Integrated Voltammetric and Chronoamperometric Study. *J. Phys. Chem.* **1994**, *98* (19), 5074−5083.
(41) Betts, A.; Briega-Martos, V.; Cuesta, A.; Herrero, E. Adsorbed Formate Is the Last Common Intermediate in the Dual-Path Mechanism of the Electrooxidation of Formic Acid. *ACS Catal.* **2020**, *10* (15), 8120−8130.
(42) Ogasawara, H.; Brena, B.; Nordlund, D.; Nyberg, M.; Pelmenschikov, A.; Pettersson, L. G. M.; Nilsson, A. Structure and Bonding of Water on Pt(111). *Phys. Rev. Lett.* **2002**, *89* (27), 276102.
(43) Raghavan, K.; Foster, K.; Berkowitz, M. Comparison of the Structure and Dynamics of Water at the Pt(111) and Pt(100) Interfaces: Molecular Dynamics Study. *Chem. Phys. Lett.* **1991**, *177* (4−5), 426−432.
(44) Zhu, J. X.; Le, J. B.; Koper, M. T. M.; Doblhoff-Dier, K.; Cheng, J. Effects of Adsorbed OH on Pt(100)/Water Interfacial Structures and Potential. *J. Phys. Chem. C* **2021**, *125* (39), 21571−21579.
(45) Del Colle, V.; Souza-Garcia, J.; Tremiliosi-Filho, G.; Herrero, E.; Feliu, J. M. Electrochemical and Spectroscopic Studies of Ethanol Oxidation on Pt Stepped Surfaces Modified by Tin Adatoms. *Phys. Chem. Chem. Phys.* **2011**, *13* (26), 12163−12172.

https://doi.org/10.1021/acssuschemeng.2c02663
ACS Sustainable Chem. Eng. 2023, 11, 4960−4968